

Enriching Neural Network Training Dataset to Improve Worst-Case Performance Guarantees

Rahul Nellikkath, Spyros Chatzivasileiadis
Department of Wind and Energy Systems
Technical University of Denmark (DTU)
Kgs. Lyngby, Denmark
{rnelli, spchatz}@dtu.dk

Abstract—Machine learning algorithms, especially Neural Networks (NNs), are a valuable tool used to approximate non-linear relationships, like the AC-Optimal Power Flow (AC-OPF), with considerable accuracy – and achieving a speedup of several orders of magnitude when deployed for use. Often in power systems literature, the NNs are trained with a fixed dataset generated prior to the training process. In this paper, we show that adapting the NN training dataset *during training* can improve the NN performance and substantially reduce its worst-case violations. This paper proposes an algorithm that identifies and enriches the training dataset with critical datapoints that reduce the worst-case violations and deliver a neural network with improved worst-case performance guarantees. We demonstrate the performance of our algorithm in four test power systems, ranging from 39-buses to 162-buses.

Index Terms—AC-OPF, Worst-Case Guarantees, Trustworthy Machine Learning, Explainable AI.

I. INTRODUCTION

Machine learning algorithms, especially Neural Networks (NNs), are a valuable tool widely used to approximate non-linear relationships with considerable accuracy. An adequately sized NN with sufficient training data can be used to estimate complex non-linear and non-convex power flow problems like the AC-Optimal Power Flow (AC-OPF) [1] in a fraction of the time it would take to solve the exact problem. Considering AC-OPF is a valuable tool that the power system operators have to use numerous times to evaluate multiple uncertain scenarios and to prepare contingency plans for the daily safe operation of the power system, a well-trained NN would be a valuable tool that can save computational time and help the power system operators run orders of magnitude more scenarios. Moreover, these well-trained NNs could be used to either replace the existing convex approximations or relaxations of these non-convex non-linear problems [2], [3], to warm start the actual problem [4], or as a surrogate function in challenging optimization algorithms [5].

However, for the widespread adoption of the NN algorithms in power systems, it is essential to build an accurate approximation of the non-linear problems that do not violate the constraints of the power system. In the case of approximating AC-OPF algorithms, a few researchers have shown that incorporating power flow constraint violations into the training process [6]–[9] can improve the accuracy of the predictions drastically. Previously, we had proposed a Physics-Informed

Neural Network (PINN) [10], which combined the KKT conditions of AC-OPF along with the power flow constraints to improve the performance of the NN [11]. Moreover, exciting research is happening on how the NN predictions could be altered to satisfy the power system constraints [12]. These works have helped improve the accuracy and build trust in the NN predictions for AC-OPF predictions.

Regardless, the performance of all these NN algorithms depends highly on the ability of the training data set to capture adverse points to the NN. Yet, a traditional NN training algorithm usually relies on a fixed training dataset, either randomly generated from the input domain or collected from a previously existing dataset, throughout the training process to generalize the problem. In a sizable system with multiple parameters to consider, one might require more than this traditional way of compiling training datasets to capture challenging adverse inputs to the NN that could lead to massive power system constraint violations once deployed. One of our previous works has shown the importance of enriching the training dataset with challenging input data points during training to improve its accuracy when predicting the N-1 small-signal stability margin of a wind farm [13].

Ultimately, to build trust in the NN's performance for a safety-critical application, such as power systems operation, some form of worst-case performance guarantees is required. Our previous work has shown how we can determine worst-case guarantees for AC [11] and DC-OPF [14] problems; and demonstrated how one could use the worst-case guarantees to select appropriate hyperparameters [11], [15] for the NN training which improve the worst-case performance. Still, as we show in this paper, we can substantially further improve the NN worst-case performance by enriching the training dataset.

In this paper, we illustrate how we can use the worst-case guarantees of the NN for AC-OPF to enrich the NN training data set with critical data points that improve the worst-case performance of the NN. Our contributions are as follows:

- 1) We demonstrate how to use the worst-case guarantees of NN predictions, proposed in [11], to enrich the NN training dataset during training to minimize the worst-case generation constraint violations of the NN.
- 2) We demonstrate how we can use a simplified MILP problem to identify the region around the point that caused worst-case constraint violations to sample effectively multiple data points to the training dataset.

This paper is structured as follows: Section II discusses AC-OPF and how we can use a power flow-informed NN

to approximate the AC-OPF solutions. Section III explains the proposed NN dataset enrichment algorithm. Section IV presents results from case studies, and Section V concludes.

II. OPTIMAL POWER FLOW ALGORITHM AND POWER FLOW INFORMED NEURAL NETWORK

This section describes the AC -OPF problem we used as a guiding application, presents the standard neural network architecture, and the power-flow-informed NN that will be used as a building block for the proposed NN training dataset enrichment algorithm.

A. AC-Optimal Power Flow

The objective function for reducing the cost of active power generation in a power system with N_g number of generators, N_b number of buses, and N_d number of loads can be formulated as follows:

$$\min_{\mathbf{P}_g, \mathbf{Q}_g, \mathbf{v}} \mathbf{c}_p^T \mathbf{P}_g \quad (1)$$

where the vector \mathbf{P}_g denotes the active power setpoints of the generators in the system, and \mathbf{c}_p^T denotes the costs vector for the active power production at each generator. \mathbf{Q}_g and \mathbf{v} denote the reactive power setpoints of the generators and the complex bus voltages, respectively. The active and reactive power injection at each node $n \in N_b$, denoted by p_n and q_n respectively, can be calculated as follows:

$$p_n = p_n^g - p_n^d \quad \forall n \in N_b, \quad (2)$$

$$q_n = q_n^g - q_n^d \quad \forall n \in N_b, \quad (3)$$

where p_n^g and q_n^g are the active and reactive power generation, and p_n^d and q_n^d are the active reactive power demand at node n . The power flow equations in the network in cartesian coordinates can be written as follows:

$$p_n = \sum_{k=1}^{N_b} v_n^r (v_k^r G_{nk} - v_k^i B_{nk}) + v_n^i (v_k^i G_{nk} + v_k^r B_{nk}) \quad (4)$$

$$q_n = \sum_{k=1}^{N_b} v_n^i (v_k^r G_{nk} - v_k^i B_{nk}) - v_n^r (v_k^i G_{nk} + v_k^r B_{nk}) \quad (5)$$

where v_n^r and v_n^i denote the real and imaginary part of the voltage at node n . The conductance and susceptance of the line nk connecting node n and k is denoted by G_{nk} and B_{nk} respectively. The power flow equations can be written in a more compact form by combining the real and imaginary parts of voltage into a vector of size $2N_b \times 1$ as $\mathbf{v} = [(\mathbf{v}^r)^T, (\mathbf{v}^i)^T]^T$ as follows [6]:

$$\mathbf{v}^T \mathbf{M}_p^n \mathbf{v} = p_n \quad \forall n \in N_b \quad (6)$$

$$\mathbf{v}^T \mathbf{M}_q^n \mathbf{v} = q_n \quad \forall n \in N_b \quad (7)$$

where \mathbf{M}_p^n and \mathbf{M}_q^n are symmetric real valued matrices [16].

The active and reactive power generation limits can be formulated as follows:

$$\underline{p}_n^g \leq p_n^g \leq \bar{p}_n^g \quad \forall n \in N_g \quad (8)$$

$$\underline{q}_n^g \leq q_n^g \leq \bar{q}_n^g \quad \forall n \in N_g \quad (9)$$

Similarly, the voltage and line current flow constraints for the power system can be represented as follows:

$$\underline{\mathbf{V}}^n \leq \mathbf{v}^T \mathbf{M}_v^n \mathbf{v} \leq \bar{\mathbf{V}}^n \quad \forall n \in N_b \quad (10)$$

$$\ell_{mn} = \mathbf{v}^T \mathbf{M}_{i_{mn}} \mathbf{v} \leq \bar{\ell}_{mn} \quad \forall mn \in N_l \quad (11)$$

where $\mathbf{M}_v^n := e_n e_n^T + e_{N_b+n} e_{N_b+n}^T$ and e_n is a $2N_b \times 1$ unit vector with zeros at all the locations except n . The squared magnitude of upper and lower voltage limit is denoted by $\bar{\mathbf{V}}^n$ and $\underline{\mathbf{V}}^n$ respectively. The squared magnitude of line current flow in line mn is represented by ℓ_{mn} and matrix $\mathbf{M}_{i_{mn}} = |y_{mn}|^2 (e_m - e_n)(e_m - e_n)^T + |y_{mn}|^2 (e_{N_b+m} - e_{N_b+n})(e_{N_b+m} - e_{N_b+n})^T$, where y_{mn} is the line admittance of branch mn . Assuming the slack bus N_{sb} acts as an angle reference for the voltage, we will have:

$$v_{N_{sb}}^i = \mathbf{v}^T \mathbf{e}_{N_b+N_{sb}} \mathbf{e}_{N_b+N_{sb}}^T \mathbf{v} = 0 \quad (12)$$

The constraints (2)-(3),(6)-(12) and the objective function for the AC-OPF problem (1) can be written in a more compact form as follows (for more details, see [6]):

$$\min_{\mathbf{v}, \mathbf{G}} \mathbf{c}^T \mathbf{G} \quad (13a)$$

$$s.t. \mathbf{v}^T \mathbf{L}_l \mathbf{v} = a_l^T \mathbf{G} + b_l^T \mathbf{D}, \quad l = 1 : L \quad (13b)$$

$$\mathbf{v}^T \mathbf{M}_m \mathbf{v} \leq d_m^T \mathbf{D} + f_m, \quad m = 1 : M \quad (13c)$$

where $\mathbf{G} = [\mathbf{P}_g^T, \mathbf{Q}_g^T]^T$, \mathbf{c}^T is the combined linear cost terms for the active power and, if necessary, reactive power generation. $\mathbf{D} = [\mathbf{P}_d^T, \mathbf{Q}_d^T]^T$ denotes the active and reactive power demand in the system. Following that, the equality constraints (6)-(7) and (12) can be represented by the $\mathbf{L} = 2N_b + 1$ constraints in (13b). Similarly, the inequality constraints (8)-(11) can be represented by the $\mathbf{M} = 4N_g + 2N_b + N_l$ constraints in (13c).

B. Neural Network for Optimal Power Flow Predictions

Neural Networks (NNs) are considered global approximators and can estimate the AC-OPF solution with significant accuracy when trained appropriately, and with sufficient training data. To achieve this, NN uses a group of interconnected hidden layers with multiple neurons to learn the relationship between the input and output layers. In the case of AC-OPF for generation cost minimization, the input layer will be the active and reactive power demand in the power system, and the output layer will be the optimal active and reactive power generation setpoints.

Each neuron in a hidden layer will be connected with neurons in the neighboring layers through a set of edges. The information exiting one neuron goes through a linear transformation before reaching the neuron in the subsequent layer. Activation functions are used in every neuron to introduce non-linear relationships into the approximator. In this paper, we use the ReLU activation function in the hidden layers, as they have shown to accelerate convergence during training [17].

A standard NN, with K number of hidden layers and N_k number of neurons in hidden layer k , is shown in Fig. 1.

The information arriving at layer k can be formulated as follows:

$$\hat{\mathbf{Z}}_k = \mathbf{w}_k \mathbf{Z}_{k-1} + \mathbf{b}_k \quad (14)$$

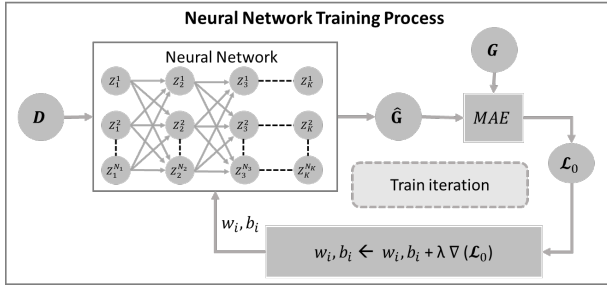


Fig. 1. Illustration of the NN training architecture to predict the optimal active and reactive power generation setpoints ($\hat{\mathbf{G}}$) using the active and reactive power demand (\mathbf{D}) in the system as input. There are K hidden layers with N_k neurons each. During training the weights \mathbf{w}_k and biases \mathbf{b}_k in the NN are optimized to minimize the average error (\mathcal{L}_0) in predicting the optimal generation setpoints (\mathbf{G}), calculated using Eq. (16). A learning rate of α controls the step size of the optimizer.

where \mathbf{Z}_{k-1} is the output of the neurons in layer $k-1$, $\hat{\mathbf{Z}}_k$ is the information received at layer k , \mathbf{w}_k and \mathbf{b}_k are the weights and biases connecting layer $k-1$ and k .

As mentioned, each neuron in the neural network uses the nonlinear ReLU activation function to accurately approximate the nonlinear relationships between the input and output layer. So, the output of each hidden layer in the NN can be represented as follows:

$$\mathbf{Z}_k = \max(\hat{\mathbf{Z}}_k, 0) \quad (15)$$

The weights \mathbf{w}_k and biases \mathbf{b}_k in the NN are optimized to minimize the average error in predicting the optimal generation setpoints in the training data set, denoted by \mathcal{L}_0 , which will be measured as follows:

$$\mathcal{L}_0 = \frac{1}{N} \sum_{i=1}^N |\mathbf{G}_i - \hat{\mathbf{G}}_i| \quad (16)$$

where N is the number of data points in the training set, \mathbf{G}_i is the generation setpoint determined by the OPF, and $\hat{\mathbf{G}}_i$ is the predicted NN generation setpoint. The back-propagation algorithm will be used to modify the weights and biases to minimize the average prediction error (\mathcal{L}_0), as shown in Fig. 1, during each iteration of the NN training. A learning rate of λ controls the step size of the optimizer.

C. Power-Flow-Informed Neural Network

A standard NN training procedure relies solely on the average error between its predictions and the data in the training dataset to achieve adequately accurate AC-OPF predictions. However, since these NN predictions should satisfy the power flow constraints given in Eq. (13), we can use a power-flow-informed NN (PFNN) similar to the ones proposed in [6], and our previous work [11] to improve the generalization capability of the NN.

The structure of the power-flow-informed NN (PFNN) used in this work is given in Fig. 2. Here an additional NN, denoted by NN_v , is used to approximate the real and imaginary part of the voltages in the system. Subsequently, both the predicted optimal generation setpoints and voltages in the system were analyzed to compute the power flow constraint violation, denoted by \mathcal{L}_{PF} , as follows:

$$\mathcal{L}_{PF} = \frac{1}{N} \sum_{i=1}^N |\sigma_{eq} + \sigma_{ineq}| \quad (17a)$$

where,

$$\sigma_{eq} = |\mathbf{v}^T \mathbf{L}_l \mathbf{v} - a_l^T \mathbf{G} - b_l^T \mathbf{D}|, \quad l = 1 : L \quad (17b)$$

$$\sigma_{ineq} = \max(\mathbf{v}^T \mathbf{M}_m \mathbf{v} - d_m^T \mathbf{D} - f_m, 0), \quad m = 1 : M \quad (17c)$$

Thus the loss function for training the PFNN is formulated as follows:

$$\mathcal{L}_{PFNN} = \Lambda_0 \mathcal{L}_0 + \Lambda_{PF} \mathcal{L}_{PF} \quad (18)$$

where Λ_0 and Λ_{PF} are the weights given to the two loss functions \mathcal{L}_0 and \mathcal{L}_{PF} , respectively.

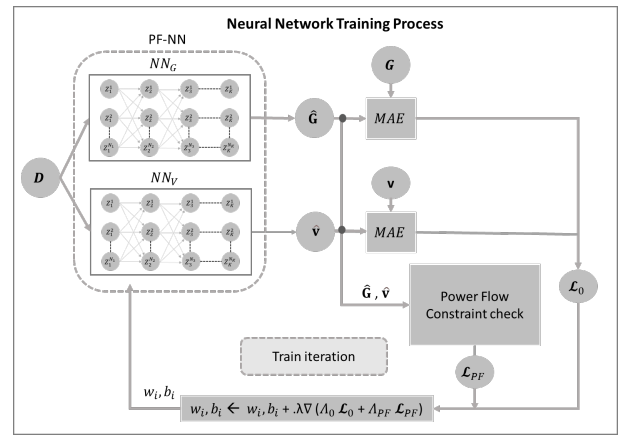


Fig. 2. Illustration of the power-flow-informed NN (PFNN) training architecture to predict the optimal active and reactive power generation setpoints ($\hat{\mathbf{G}}$) using the active and reactive power demand (\mathbf{D}) in the system as input. There are two NNs, one for predicting $\hat{\mathbf{G}}$, denoted by NN_G , and the other for predicting the voltage in the system, denoted by NN_v . During training, the weights \mathbf{w}_k and biases \mathbf{b}_k in the NN are optimized to minimize the average error (\mathcal{L}_0) in predicting the optimal generation (\mathbf{G}) and voltage setpoints (\mathbf{v}), and the power flow constraint violation (\mathcal{L}_{PF}). See (17) for the calculations.

In our investigations, this configuration of NN with power flow constraint check has been shown to improve the average and worst-case performance of the NN without introducing a substantial computational burden. Still, the performance of the trained PFNN depends highly on the ability of the training dataset to capture adverse points to the PFNN.

III. NEURAL NETWORK DATA ENRICHING USING WORST-CASE CONSTRAINT VIOLATIONS

The following section describes a NN dataset-enriching algorithm that uses worst-case generation constraint violations in regular intervals during training to identify the input regions causing the largest generation constraint violations and then enrich the training dataset with new training points from those regions. This shall help minimize the probability a NN prediction to lead to significant generation constraint violations.

A. Worst-Case Violations of the Neural Networks to Identify Adverse Examples

As mentioned earlier, we determine the input data with which we enrich our NN training dataset by identifying which are the NN inputs that cause the worst violations. The optimization problem to identify worst-case generation constraint violation is presented in (19) [11]:

$$\max_{\mathbf{D}} v_g \quad (19a)$$

$$v_g = \max_{\mathbf{D}}(\hat{\mathbf{G}} - \overline{\mathbf{G}}, \underline{\mathbf{G}} - \hat{\mathbf{G}}, 0) \quad (19b)$$

$$\text{s.t. (14), (15)} \quad (19c)$$

where $\overline{\mathbf{G}}$ and $\underline{\mathbf{G}}$ are the maximum and minimum active and reactive power generation bounds. However, the formulation for the ReLU activation function in (15) is nonlinear. So, the ReLU activation function is reformulated into a set of mixed-integer linear inequality constraints, as follows, to simplify the optimization problem [14]:

$$\mathbf{Z}_k = \max(\hat{\mathbf{Z}}_k, 0) \Rightarrow \begin{cases} \mathbf{Z}_k \leq \hat{\mathbf{Z}}_k - \underline{\mathbf{Z}}_k(1 - \mathbf{y}_k) & (20a) \\ \mathbf{Z}_k \geq \hat{\mathbf{Z}}_k & (20b) \\ \mathbf{Z}_k \leq \overline{\mathbf{Z}}_k \mathbf{y}_k & (20c) \\ \mathbf{Z}_k \geq \mathbf{0} & (20d) \\ \mathbf{y}_k \in \{0, 1\}^{N_k} & (20e) \end{cases}$$

where \mathbf{Z}_k and $\hat{\mathbf{Z}}_k$ are the outputs and inputs of the ReLU activation function, y_k^i is a binary variable, and $\underline{\mathbf{Z}}_k$ and $\overline{\mathbf{Z}}_k$ are the upper and lower limits of the input to ReLU. These limits should be sufficiently large to ensure they are not binding and small enough so the constraints are not unbounded. We used interval arithmetic to ensure a tighter bound (ref [18] and [14] for more information). If $\hat{\mathbf{Z}}_k$ is less than zero, then y_k^i will be zero because of (20c), and Z_k^i will be constrained to zero. Else, y_k^i will be equal to one, and Z_k^i will be equal to $\hat{\mathbf{Z}}_k$ due to (20a) and (20b).

The MILP optimization problem for identifying the specific input combination that could lead to a large generation constraint violation (will be denoted by D_{WC} from now on) can be formulated as follows:

$$\max_{\mathbf{D}} v_g \Rightarrow v_g^{max} \quad (21a)$$

$$v_g = \max(\hat{\mathbf{G}} - \overline{\mathbf{G}}, \underline{\mathbf{G}} - \hat{\mathbf{G}}, 0) \quad (21b)$$

$$\text{s.t. (14), (20)} \quad (21c)$$

where v_g^{max} is the worst-case generation constraint violation obtained after solving the optimization.

By solving the optimization problem mentioned above for all the generators in the system, we can identify the specific D_{WC} that caused the largest constraint violations. However, simply adding these D_{WC} to the dataset might not be adequate; instead, to properly enrich the dataset, it is also essential to identify the size of a region around D_{WC} that could lead to equally large constraint violations. Thus, we can collect multiple points from this region to enrich the dataset.

The optimization problem below is used to fit a hypercube to the space around D_{WC} that could cause significant constraint violations.

$$\max_{\mathbf{D}} d \quad (22a)$$

$$d = \|D_0 - D_{WC}\|_{\infty} \quad (22b)$$

$$\text{s.t. } v_g \geq \alpha \cdot v_g^{max} \quad (22c)$$

$$(14), (20) \quad (22d)$$

Here, the distance d defines a hypercube around D_{WC} that causes constraint violations more than $\alpha \cdot v_g$. We can choose a smaller or larger value of α to get a wider or tighter region around D_{WC} .

In the optimization problem (22), for α close to 1, we can assume the hypercube around D_{WC} will be small. Thus we can consider a significant positive or negative $\hat{\mathbf{Z}}$ value will not change signs for any of the input data points inside the hypercube. Therefore, we can set those ReLU statuses, denoted by \mathbf{y}_k in (20), to always be active or inactive in the hypercube. This reduces the number of binary variables in the optimization problem and thereby reduces the computational complexity of the optimization problem. A threshold of 10 % with respect to the $\overline{\mathbf{Z}}$ or $\underline{\mathbf{Z}}$ was used to decide whether to fix \mathbf{y}_k or not. That is, if the $\overline{\mathbf{Z}}$ value for NN input D_{WC} was more than $0.1 \cdot \overline{\mathbf{Z}}$ or less than of $0.1 \cdot \underline{\mathbf{Z}}$, then those binary variables are set to active or inactive respectively in the hypercube.

After obtaining the size of the hypercube, a random gaussian sampling, centered at D_{WC} , is used to sample new training data points from the hypercube. Unlike the original training dataset, we did not compute the optimal generation setpoints (i.e., \mathbf{G}) for these additional data points to avoid using extra computational power to solve the AC-OPF problem. Instead, we used the power flow constraint violations in \mathcal{L}_{PF} to train the neural network.

The proposed NN dataset enrichment algorithm is given in Algorithm 1.

IV. RESULTS & DISCUSSION

This section compares the worst-case generation constraint violations and the average performance of an NN with the proposed training dataset enrichment algorithm, denoted by WC-PFNN, against the power-flow-informed NN (PFNN) which uses a fixed training dataset. The results are analyzed for AC-OPF on 4 test systems: the 39-bus, 57-bus, 118-bus, and 162-bus systems from PGLib-OPF network library v19.05 [19]. The test system characteristics are given in Table I.

In all instances, the input region for the active and reactive power demand was assumed to be convex, and at each node, the active and reactive power demand was considered to be between 60% to 100% of their respective nominal loading. This is a reasonable assumption used to simplify the dataset generation process. To give an idea about the size of each system, the sum of the maximum loading over all nodes for each system is given in Table I.

While generating the training data points, each node's active and reactive power demand was assumed to be independent. Then, for all cases, 10'000 sets of random input demand values were picked from the input domain using Latin hypercube sampling [20]. From these, 50% were allocated to the training

Algorithm 1 Proposed NN Dataset Enriching algorithm

- 1: TRAIN(w_i, b_i)
- 2: Initialize the NN weights (w_i) and biases (b_i)
- 3: Set the learning rate (α), total number of epochs (T), number of iterations before accessing the worst-case violations to enrich the dataset for the first time (T_{int}) and number of iterations before enriching the dataset again (T_{enr})
- 4: initialize $t=1$
- 5: Repeat
- 6: Calculate average losses \mathcal{L}_0 and \mathcal{L}_{PF} in the training dataset
- 7: Update NN weights and biases w_i and b_i using the back propagation algorithm as follows:
 $w_i, b_i = w_i, b_i + \alpha \nabla (\Lambda_0 \mathcal{L}_0 + \Lambda_{PF} \mathcal{L}_{PF})$
- 8: $t=t+1$
- 9: until $t = T_{int}$
- 10: Repeat
- 11: initialize $t_{enr} = 1$
- 12: Solve MILP optimization given in Eq. (19) is used to get the worst-case generation constraint violation v_g^{max} and D_{WC}
- 13: Solve MILP optimization given in Eq. (22) is used to get the hyper-cube around D_{WC} and sample new data points from those hyper-cubes. Add these new points to the training set
- 14: Repeat
- 15: Calculate average losses \mathcal{L}_0 and \mathcal{L}_{PF} in the training dataset
- 16: Update NN weights and biases w_i and b_i using the back propagation algorithm as:
 $w_i, b_i = w_i, b_i + \alpha \nabla (\Lambda_0 \mathcal{L}_0 + \Lambda_{PF} \mathcal{L}_{PF})$
- 17: $t_{enr} = t_{enr} + 1$
- 18: $t=t+1$
- 19: until $t_{enr} = T_{enr}$
- 20: until $t = T$

TABLE I
TEST CASE CHARACTERISTICS

Test Case	N_b	N_d	N_g	N_l	Max total load	
					MW	MVA
case39	39	21	10	46	6254	6626
case57	57	42	4	80	1251	1375
case118	118	99	19	186	4242	4537
case162	162	113	12	284	7239	12005

dataset, 20% were assigned to the validation set, and the remaining 30% were assigned to the unseen test dataset. The AC-OPF solver in MATPOWER [21] was used to obtain the optimal generation setpoints and the voltages at each bus.

A NN with three hidden layers and 20 nodes in each layer is used to predict the AC-OPF solutions. The ML algorithms were implemented using PyTorch [22] and the Adam optimizer [23]; a learning rate of 0.001 was used for training. WandB [24] was used for monitoring and tuning the hyperparameters. The MILP problem for obtaining the worst-case violations and

identifying the region was programmed in Pyomo [25] and solved using the Gurobi solver [26]. The NNs were trained in a High-Performance Computing (HPC) server with an Intel Xeon E5-2650v4 processor and 256 GB RAM. The code and datasets to reproduce the results are available online [27].

A. Comparing the Average and the Worst-Case Performance

Both the PFNN and WC-PFNN algorithms, in all cases, achieved convergence in 600 iterations. After every 200 iterations during training, we evaluated the worst-case constraint violations, and in the case of WC-PFNN, a new 1000 data points were added to the training dataset. To compensate, 2000 random data points were added to the PFNN training dataset before starting the training process to have a comparable training dataset.

For WC-PFNN and PFNN, we selected the weight Λ_0 and Λ_{PF} for the loss functions L_0 and L_{PF} that offered the lowest worst-case generation constraint violation using WandB.

While comparing the worst-case performance over the training process, we can see in Fig. 3 that in all cases, the proposed NN dataset enriching algorithms (WC-PFNN) result in a steep reduction in worst-case guarantees. At the same time, the PFNN was only able to achieve a slight decline or, in case162 and case 57, even an increase in worst-case generation constraint violation during training. This highlights the importance of monitoring and enriching the NN dataset using worst-case constraint violations.

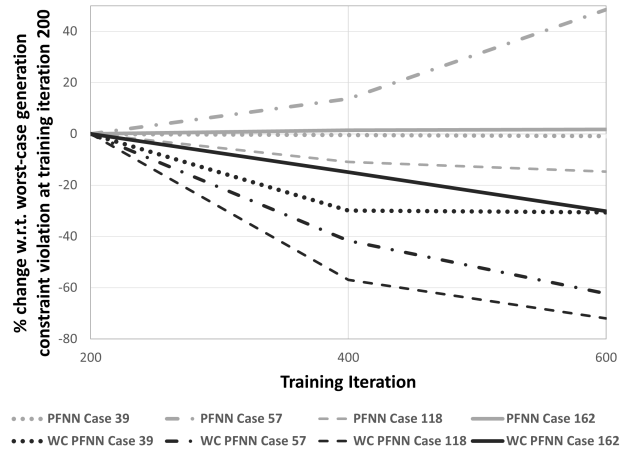


Fig. 3. Change in worst case generation constraint violation with respect to the worst-case generation constraint violation at training iteration 200

The mean absolute error (MAE) in an unseen test dataset, the worst-case generation constraint violation (v_g), and the width of the hypercube around D_{WC} , denoted by d (as a fraction of the nominal loading at each node), caused by PFNN and WC-PFNN after training are given in Table II.

From Table II, we see that WC-PFNN can reduce worst-case generation constraint violations by more than 30% in all test systems. As a matter of fact, in case57, it achieves an up to 80% reduction compared to PFNN with a fixed dataset. Moreover, it was observed that the hypercube around D_{WC} , which collects points that could cause significant constraint violations (see (22)), was also shrinking as we were including new points in the training set. So, the proposed method also made the NN safer in more regions in the input domain.

TABLE II
AVERAGE AND WORST-CASE PERFORMANCE

Test Case		MAE (%)	v_g (MVA)	d
Case 39	PFNN	0.56	6.08	0.03
	WC-PFNN	0.52	4.18	0.02
Case 57	PFNN	1.2	1280	0.05
	WC-PFNN	1.1	304	0.01
Case 118	PFNN	0.36	1879	0.04
	WC-PFNN	0.35	600	0.02
Case 162	PFNN	1.4	7552	0.03
	WC-PFNN	1.2	5212	0.02

V. CONCLUSION

The objective of this paper is to demonstrate the importance of enriching the NN training dataset with critical datapoints in order to improve the NN worst-case performance. To determine these datapoints we use algorithms that accurately quantify the worst-case violations of the NN. This helps significantly improve the NN performance and enhances the trust in NN for safety-critical applications. In this paper, we show that by enriching the NN training dataset using the worst-case generation constraint violations of an AC-OPF problem during training, we can improve the worst-case performance of the NN drastically. We test the proposed algorithm on four different power systems, ranging from 39-buses to 162-buses and we show that we can achieve up to 80% reduction in worst-case performance. In future work, we plan to integrate this approach with our recent work on designing a neural network training procedure that achieves best average performance and minimizes the worst case violations at the same time [28].

REFERENCES

- [1] D. K. Molzahn and I. A. Hiskens, "A survey of relaxations and approximations of the power flow equations," *Foundations and Trends® in Electric Energy Systems*, vol. 4, no. 1-2, pp. 1–221, 2019.
- [2] S. H. Low, "Convex relaxation of optimal power flow—part i: Formulations and equivalence," *IEEE Transactions on Control of Network Systems*, vol. 1, no. 1, pp. 15–27, 2014.
- [3] A. Venzke, S. Chatzivasileiadis, and D. K. Molzahn, "Inexact convex relaxations for ac optimal power flow: Towards ac feasibility," *Electric Power Systems Research*, vol. 187, p. 106480, 2020.
- [4] L. Zhang and B. Zhang, "Learning to solve the ac optimal power flow via a lagrangian approach," *arXiv preprint arXiv:2110.01653*, 2021.
- [5] A. Kody, S. Chevalier, S. Chatzivasileiadis, and D. Molzahn, "Modeling the ac power flow equations with optimally compact neural networks: Application to unit commitment," *Electric Power Systems Research*, vol. 213, p. 108282, 2022.
- [6] M. Singh, V. Kekatos, and G. B. Giannakis, "Learning to solve the ac-opf using sensitivity-informed deep neural networks," *IEEE Transactions on Power Systems*, pp. 1–1, 2021.
- [7] F. Fioretto, T. W. Mak, and P. Van Hentenryck, "Predicting ac optimal power flows: Combining deep learning and lagrangian dual methods," in *Proceedings of the AAAI Conference on Artificial Intelligence*, vol. 34, no. 01, 2020, pp. 630–637.
- [8] X. Pan, T. Zhao, and M. Chen, "Deepopf: Deep neural network for dc optimal power flow," in *2019 IEEE International Conference on Communications, Control, and Computing Technologies for Smart Grids (SmartGridComm)*. IEEE, 2019, pp. 1–6.
- [9] P. L. Donti, D. Rolnick, and J. Z. Kolter, "Dc3: A learning method for optimization with hard constraints," *arXiv preprint arXiv:2104.12225*, 2021.
- [10] M. Raissi, P. Perdikaris, and G. Karniadakis, "Physics-informed neural networks: A deep learning framework for solving forward and inverse problems involving nonlinear partial differential equations," *Journal of Computational Physics*, vol. 378, pp. 686–707, 2019. [Online]. Available: <https://www.sciencedirect.com/science/article/pii/S0021999118307125>
- [11] R. Nellikkath and S. Chatzivasileiadis, "Physics-Informed Neural Networks for AC Optimal Power Flow," *Electric Power Systems Research*, vol. 212, p. 108412, 2022. [Online]. Available: <https://www.sciencedirect.com/science/article/pii/S0378779622005636>
- [12] P. L. Donti, D. Rolnick, and J. Z. Kolter, "Dc3: A learning method for optimization with hard constraints," *arXiv preprint arXiv:2104.12225*, 2021.
- [13] J. Stiasny, S. Chevalier, R. Nellikkath, B. Sævarsson, and S. Chatzivasileiadis, "Closing the loop: A framework for trustworthy machine learning in power systems," in *Proceedings of 11th Bulk Power Systems Dynamics and Control Symposium (IREP 2022)*, 2022, 11th Bulk Power Systems Dynamics and Control Symposium, IREP'2022 ; Conference date: 25-07-2022 Through 30-07-2022.
- [14] A. Venzke, G. Qu, S. Low, and S. Chatzivasileiadis, "Learning optimal power flow: Worst-case guarantees for neural networks," in *2020 IEEE International Conference on Communications, Control, and Computing Technologies for Smart Grids (SmartGridComm)*. IEEE, 2020, pp. 1–7.
- [15] R. Nellikkath and S. Chatzivasileiadis, "Physics-Informed Neural Networks for Minimising Worst-Case Violations in DC Optimal Power Flow," in *2021 IEEE International Conference on Communications, Control, and Computing Technologies for Smart Grids (SmartGridComm)*, 2021, pp. 419–424.
- [16] V. Kekatos, G. Wang, H. Zhu, and G. B. Giannakis, "Psse redux: convex relaxation, decentralized, robust, and dynamic solvers," *Advances in Electric Power and Energy: Static State Estimation*, pp. 171–208, 2020.
- [17] A. B. X. Glorot and Y. Bengio, "Deep sparse rectifier neural networks," in *Proceedings of the fourteenth international conference on artificial intelligence and statistics*. JMLR Workshop and Conference Proceedings, 2011, pp. 315–323.
- [18] V. Tjeng, K. Xiao, and R. Tedrake, "Evaluating robustness of neural networks with mixed integer programming," *arXiv preprint arXiv:1711.07356*, 2017.
- [19] S. Babaeinejadsarookolae, A. Birchfield, R. D. Christie, C. Coffrin, C. DeMarco, R. Diao, M. Ferris, S. Fliscounakis, S. Greene, R. Huang *et al.*, "The power grid library for benchmarking ac optimal power flow algorithms," *arXiv preprint arXiv:1908.02788*, 2019.
- [20] M. D. McKay, R. J. Beckman, and W. J. Conover, "A comparison of three methods for selecting values of input variables in the analysis of output from a computer code," *Technometrics*, vol. 42, no. 1, pp. 55–61, 2000.
- [21] R. D. Zimmerman, C. E. Murillo-Sánchez, and R. J. Thomas, "Matpower: Steady-state operations, planning, and analysis tools for power systems research and education," *IEEE Transactions on power systems*, vol. 26, no. 1, pp. 12–19, 2010.
- [22] A. Paszke, S. Gross, F. Massa, A. Lerer, J. Bradbury, G. Chanan, T. Killeen, Z. Lin, N. Gimelshein, L. Antiga, A. Desmaison, A. Kopf, E. Yang, Z. DeVito, M. Raison, A. Tejani, S. Chilamkurthy, B. Steiner, L. Fang, J. Bai, and S. Chintala, "Pytorch: An imperative style, high-performance deep learning library," in *Advances in Neural Information Processing Systems 32*, H. Wallach, H. Larochelle, A. Beygelzimer, F. d'Alché-Buc, E. Fox, and R. Garnett, Eds. Curran Associates, Inc., 2019, pp. 8024–8035. [Online]. Available: <http://papers.nips.cc/paper/9015-pytorch-an-imperative-style-high-performance-deep-learning-library.pdf>
- [23] D. P. Kingma and J. Ba, "Adam: A method for stochastic optimization," in *3rd International Conference on Learning Representations, ICLR 2015, San Diego, CA, USA, May 7-9, 2015, Conference Track Proceedings*, Y. Bengio and Y. LeCun, Eds., 2015. [Online]. Available: <http://arxiv.org/abs/1412.6980>
- [24] L. Biewald, "Experiment tracking with weights and biases," 2020, software available from wandb.com. [Online]. Available: <https://www.wandb.com/>
- [25] M. L. Bynum, G. A. Hackebeil, W. E. Hart, C. D. Laird, B. L. Nicholson, J. D. Siirrola, J.-P. Watson, and D. L. Woodruff, *Pyomo—optimization modeling in python*, 3rd ed. Springer Science & Business Media, 2021, vol. 67.
- [26] Gurobi Optimization, LLC, "Gurobi Optimizer Reference Manual," 2022. [Online]. Available: <https://www.gurobi.com>
- [27] R. Nellikkath and S. Chatzivasileiadis, "Supplementary data and code: Enriching neural network training dataset to improve worst-case performance guarantees," 2022. [Online]. Available: https://github.com/RahulNellikkath/Enriching_Neural_Network_Dataset
- [28] —, "Minimizing worst-case violations of neural networks," *arXiv preprint arXiv:2212.10930*, 2022.